ELSEVIER

Coordination Chemistry Reviews
177 (1998) 37–60

COORDINATION CHEMISTRY REVIEWS

Solvent effects on metal to ligand charge transfer excitations

N.S. Hush [a,b], J.R. Reimers [a,*]

[a] *School of Chemistry, University of Sydney, Sydney, NSW 2006, Australia*
[b] *Department of Biochemistry, University of Sydney, Sydney, NSW 2006, Australia*

Received 29 September 1997; received in revised form 21 January 1998; accepted 3 March 1998

Contents

Abstract

The method for calculating solvent shifts on metal to ligand charge transfer (MLCT) and other electronic absorption bands involving charge transfer (e.g. ligand to metal and organic charge transfer) developed by Zeng, Hush and Reimers, henceforth named ZHR-SS, is reviewed. Also included are simple models for MLCT processes in mono- and di-metal complexes and a description of key aspects of modern electroabsorption spectroscopic techniques used to study MLCT transitions. The rationale behind ZHR-SS is summarized, as

* Corresponding author. Fax: +61 2 93513329; e-mail: reimers@chem.usyd.edu.au

PII S0010-8545(98)00100-3

are other schemes currently available for the evaluation of solvent effects on electronic spectra. Initial test calculations are described in which ZHR-SS is used to predict solvent effects on (n, π^*) transitions of azines: the physical processes involved closely resemble those involved in MLCT spectra, but a much larger range of experimental data is available to test the method. Results for MLCT and related processes in $Fe^{2+}(H_2O)_6$, $Ru^{2+}(NH_3)_5$–pyridine, $Ru^{2+}(NH_3)_5$–pyrazine, and $Ru^{2+}(NH_3)_5$–pyrazine-H^+ are described which accommodate the (initially surprising) results of electroabsorption experiments within the general physical picture of MLCT processes.

Keywords: Metal to ligand charge transfer; Solvent shift; Mono- and di-metal complexes

1. Introduction

While most techniques for the prediction of electronic spectra apply to molecules in the gas phase, most experiments, and in particular those relating to inorganic complexes, are performed in solution or some other condensed phase. If a significant charge rearrangement is associated with the electronic transition, then in polar media sizeable electrostatic interactions between the solute and solvent molecules occur, and these can produce large solvent (solvatochromatic) shifts $\Delta\nu$ of electronic absorption bands. They also modulate the electronic redistribution associated with the transition, as manifest e.g. through the observed change in dipole moment $\Delta\mu$ caused by the transition. For a long time there has been much interest in the interpretation of observed solvatochromatic shifts, with earlier models treating the solvent implicitly using a dielectric continuum [1–7]. Indeed, important conclusions concerning the physical origins of emission spectra and the nature of hydrogen bonding were drawn from the results [8,9]. Recently, experimental studies of the change in dipole moment on absorption have become important; these electroabsorption studies were stimulated by the pioneering work of Boxer and coworkers [10,11] who showed that it is possible to extract intricate details of processes such as electron transfer after photoabsorption within naturally occurring photosynthetic reaction centres as well as metal to ligand charge transfer (MLCT) processes in inorganic complexes. Whereas the solvent effect on $\Delta\nu$ amounts to typically only a small fraction of ν itself, the solvent effect on $\Delta\mu$ can be of the same order as the free molecule value. The primary aim of the work reviewed here on the spectroscopy of coordination complexes was to understand quantitatively the results of Boxer's experiments on MLCT absorption: the results detail the interactions between inorganic complexes and an aqueous solvent.

From the beginning it was clear [12] that the experimental results for $\Delta\mu$ for MLCT bands imply much smaller amounts of electron transfer than are depicted in the standard physical model for such transitions. In this model, light absorption causes an electron to leave a 'donor' molecular fragment, travel a macroscopic distance large compared to the fragment size, and end up located on an 'acceptor'

fragment: for MLCT, the donor is the metal and the acceptor is the ligand, but the roles simply reverse for ligand to metal charge transfer (LMCT). The change in the total dipole moment of the system is then given simply by:

$$\Delta\mu = er_0 \tag{1}$$

where e is the magnitude of the charge on the electron and r_0 is the distance between the centres of the donor and acceptor fragments. For large ligands such as 4,4′-bipyridine, the observed $\Delta\mu$ is close to (but less than) this value, while for small ligands such as pyridine and pyrazine, $\Delta\mu$ is often only one quarter of the expected value. We [12] attributed this to a combination of back-bonding, polarization, and environmental effects arising from surrounding ligands and solvent. Subsequently, we developed the quantitative ZHR-SS method [13–22] through which these effects could be accessed quantitatively.

The original study of Oh et al. [11] revealed the electroabsorption spectra of $Ru^{2+}(NH_3)_5$–pyrazine, $Ru^{2+}(NH_3)_5$–pyrazine-H^+, the Creutz–Taube ion and other bisruthenium complexes. Other inorganic ruthenium complexes have recently been studied at Brookhaven [23], and more studies are currently under way in various research laboratories. Basically, these experiments proceed by applying a very large electric field to a thin sample held dilute in a glass (e.g. glycerol–water) at 100 K. The change in the absorption spectrum as a function of the applied field is detected, the field-dependent absorption bandshape ε/ν for each molecule in the sample being expressed as:

$$\frac{\varepsilon}{\nu}(\boldsymbol{F}, \nu) = \frac{|\boldsymbol{M}(\boldsymbol{F})|^2}{|\boldsymbol{M}(\boldsymbol{0})|^2} \times \frac{\varepsilon}{\nu}(\boldsymbol{0}, \nu + \Delta\nu) \tag{2}$$

where $\varepsilon(0, \nu)$ is its field-free absorption spectrum

$$\Delta\nu = -\Delta\boldsymbol{\mu} \cdot \boldsymbol{F} - \boldsymbol{F} \cdot \frac{\Delta\boldsymbol{\alpha}}{2} \cdot \boldsymbol{F} \tag{3}$$

provides a uniform translation of its absorption band in frequency, $\Delta\boldsymbol{\mu}$ is the (vector) change in dipole moment induced by the transition, $\Delta\boldsymbol{\alpha}$ is the corresponding (tensor) change in polarizability, $\boldsymbol{F}$ is the local applied field at the molecule, and $\boldsymbol{M}(\boldsymbol{F})$ is the field-dependent electronic transition moment expressed as:

$$\boldsymbol{M}(\boldsymbol{F}) = \boldsymbol{M}(\boldsymbol{0}) + \boldsymbol{A} \cdot \boldsymbol{F} + \boldsymbol{F} \cdot \boldsymbol{B} \cdot \boldsymbol{F} \tag{4}$$

where $\boldsymbol{A}$ is the transition moment polarizability tensor and $\boldsymbol{B}$ the transition moment hyperpolarizability third-rank tensor. A thorough theory for this effect has been developed by Liptay [24–27] and important features summarized [11,12]. In principle, all of the components of $\Delta\boldsymbol{\mu}$, $\Delta\boldsymbol{\alpha}$, $\boldsymbol{A}$, and $\boldsymbol{B}$ contribute to spectra and could be determined experimentally. This is difficult to achieve in practice, however, with typically only $|\Delta\boldsymbol{\mu}|$ and $\Delta\boldsymbol{\mu} \cdot \boldsymbol{M}$ being attained easily [11]. Fortunately, $|\Delta\boldsymbol{\mu}|$ and $\Delta\boldsymbol{\mu} \cdot \boldsymbol{M}$ are important quantities which provide key information concerning the nature of the excited state, information not obtained easily by other means, making electroabsorption spectroscopy an attractive endeavour.

Theoretically, it is possible to evaluate all of the tensor quantities involved and hence predict the observed electroabsorption spectra. We have chosen not to follow this path, but rather to introduce an analytical approximation which serves to dramatically reduce the number of molecular parameters involved and hence provide a simple means of inverting the experimental data to determine molecular parameters. MLCT transitions involve long-range electron transfer and so $\Delta\boldsymbol{\mu}$ is strongly directed between the centres of the donor and acceptor functionalities; similarly, $\Delta\boldsymbol{\alpha}$, $\boldsymbol{A}$, and $\boldsymbol{B}$ are also dominated by the single tensor component in this direction. Hence, our approximation is to replace the tensors $\Delta\boldsymbol{\mu}$, $\Delta\boldsymbol{\alpha}$, $\boldsymbol{A}$, and $\boldsymbol{B}$ with scalars $\Delta\mu$, $\Delta\alpha$, A, and B, respectively. Of course this approximation can only be meaningful if $\Delta\boldsymbol{\mu}$ and $\boldsymbol{M}$ are parallel, and indeed this has been verified experimentally for MLCT transitions [11,23]. Under these circumstances, standard electroabsorption experimental techniques yield three independent physical results (being coefficients of the zeroth, first and second derivatives of the absorption bandshape [12,24–27]), insufficient [12] to uniquely determine all of the four remaining fundamental molecular properties $\Delta\mu$, $\Delta\alpha$, A, and B. Only $|\Delta\mu|$ is determined unambiguously.

Recent experimental innovations in electroabsorption spectroscopy introduced by Chattopadhyay and Boxer [28] have widened the applicability of the technique from largely electron transfer driven electronic transitions to simple vibrational transitions in arbitrary molecules. We have developed a comprehensive analytical theory to describe these spectra [29], and applied it to simple molecules [30]. Somewhat surprisingly, the conclusions drawn from these studies strongly parallel those drawn from MLCT studies: in both the electronic and vibrational cases, the solvent shift and observed dipole moment changes are dominated by specific solvation effects involving hydrogen bonding between ionic or polar chromophores and aqueous-based solvents. This work is beyond the scope of this review, however.

Our first studies concerned the basic physical features of MLCT transitions in mono-metal [12] and bis-metal [31] complexes. These are reviewed in Section 2, including a discussion of delocalized versus localized MLCT transitions in bis-metal complexes, showing how electroabsorption spectroscopy can unambiguously discriminate between the two possibilities. We also considered the qualitative origins of solvent effects on MLCT transitions, and this is reviewed in Section 3.

Our next step was to develop methods for the quantitative interpretation of the experimental results. This was achieved in two steps: first modelling the properties of the complexes in the gas phase, and then modelling the solvent effects on the MLCT transitions. Methods for modelling the solvent effects [32] can be separated into three broad categories: those that treat the solvent implicitly using reaction-field technology, those that treat the solvent as explicit molecules, and those that employ statistical mechanics techniques [33].

Reaction field techniques [34–40] treat the solvent as a dielectric continuum containing a cavity in which the chromophore lies. These methods can qualitatively describe many features of solvation. They can readily be applied to a large range of solvents, but the shape of the solvent cavity is arbitrary and the results obtained tend to be very sensitive to cavity shape and size. In qualitative studies this can be

exploited, introducing cavity shape parameters to which experimental results are fitted. Modern approaches [40] use prespecified cavity definitions, and solve the electronic structure of the chromophore self-consistently with the reaction field generated by the cavity; these have been very successful. They cannot, however, be applied directly and quantitatively in scenarios featuring strong specific interactions between the solvent and solute, but can be used successfully in supramolecular calculations [41]. Specific solvent interactions result in solvent molecules placed at specific locations relative to the solute, and can even evoke chemical effects such as charge transfer with the solvent. Clearly, specific solvation effects could be very important for inorganic complexes (and, in general, for any system involving significant charge transfer), and hence these approaches were not employed. An example of a reaction-field calculation for MLCT spectral properties is that of Broo and Larsson [42]; while qualitative features are reproduced, issues affecting the method used to describe the solvent (e.g. 'cavity radii') make quantitative analysis impossible.

Methods which involve explicit solvent molecules are usually termed supramolecular; there has been a large variety of methods suggested for the implementation of such schemes [43–50]. Two steps are always involved, either implicitly or explicitly: the determination of the solvent structure, and the determination of the (MLCT) spectrum as a function of the solvent structure.

One of the most conceptually appealing schemes for determining the solvent structure is the Carr–Parinello density functional molecular dynamics scheme [51]. This determines the solvent structure using a high level of electronic structure theory, treating all solvent and solute molecules equivalently. Of course, the disadvantage of this approach is the enormous computational resources required, and such schemes are not currently feasible for the study of MLCT spectra.

A variety of more approximate schemes have been generated, the most promising of which include Warshell's generalized solvation models [52], hybrid quantum mechanics/molecular mechanics (QM/MM) schemes [45,48], and even simpler simulation methods [53]. These treat the chromophore and critical solvent molecules using a high level of theory and the peripheral solvent molecules using more approximate schemes. A scheme of this type has been applied by Zerner and coworkers to study inorganic MLCT [49] and other [34,35] transitions. This places the solute and a small number of solvent molecules inside a solvent cavity. It has the advantage that it includes all interactions (including charge transfer and dispersion) between the solvent and solute, but the implementation has been restricted by the need to employ the semi-empirical INDO technique in an inappropriate manner [20], and has been restricted to structures at 0 K.

We choose not to follow these schemes largely because preliminary calculations indicate that the results are unreliable in that errors arising from the approximations used to solve the electronic structure could not be controlled. Instead, we developed a simpler model, herein abbreviated as ZHR-SS, which will ultimately be limited by the difficulty in reducing its error bars, but in which the errors can be controlled and hence reliability established.

ZHR-SS is summarized in Section 4. It involves four independent steps, with the results of each step being independently verifiable by comparison of the results with experimental data. In this way, computation of (say) the solvent effects on an MLCT band is not performed in isolation but arises as one element of a broad ranging model for the spectroscopic, electronic and geometric properties of the chromophore and the solution. Briefly, the steps involve:

1. determining the electronic structure and spectroscopy of the chromophore in the gas phase;
2. determining force fields through which the chromophore interacts with the solvent;
3. determining the structure of the solution; and
4. determining the effect of the solvent structure on the electronic transition of the chromophore.

We find that, in general, only when the electronic structure of the chromophore in its ground electronic state in the gas phase is correctly described is it possible to generate an accurate force field which can predict known properties of the solution, and only when the solution structure is correctly described can the solvent effects on the chromophore be reliably obtained. A subtle but important feature that emerged [20,22] is that solvation also affects the geometry of a complex, and it is important that step 1 be performed at a realistic solution phase geometry.

While our method embodies a variety of options concerned primarily with choice of electronic structure method, the specification of the intermolecular potential functions, and technical issues such as the choice of boundary conditions used in the computer simulations, and while it requires the determination of a significant number of properties of the solvent and solute molecules in the gas phase, it contains no parameters which can arbitrarily be adjusted in order to fit experimental spectroscopic data.

Our initial applications of ZHR-SS were not to inorganic MLCT spectra and the like as the detailed experimental information required to verify steps 1–4 above is typically not available. Instead, we modelled the solvent effects on the (n, π^*) spectra of simple azines (pyridine [13], pyrazine [19], pyrimidine [14–16], and pyridazine [21]) in aqueous solution, and this work is reviewed in Section 5. These molecules were chosen because their study was very important in the determination over 40 years ago of the basic properties of hydrogen bonding, a large amount of experimental data (including high-resolution gas phase spectroscopy) is available, the molecules are small enough to treat with very accurate ab initio methods such as complete active space self-consistent field theory followed by multi-reference configuration interaction (CASSCF-MRCI), the spectroscopy of many azine–water clusters is known, the solvent shifts are relatively small (ca. 3000 cm^{-1}) so that these molecules pose difficult test cases, and qualitatively the same chemical effects apply to these molecules (even issues of localization/delocalization of the excitation), as well as to MLCT transitions in inorganic complexes.

We suggest that the success of ZHR-SS in modelling the detailed experimental information available for solvation of azines acts as a credential for the model when applied to inorganic MLCT spectra. The same cannot be said for other methods

[49] used for modelling solvent effects on MLCT spectra for which the corresponding studies on azines produce qualitatively rather poor results [34,35]. The method in question here is a supramolecular method which employs INDO to determine the solvent near-solute interactions and a dielectric continuum for more distant solvent molecules. While INDO remains the only practicable method for determining spectroscopic properties of molecules containing more than a dozen atoms, it describes properties such as intermolecular hydrogen bonding quite poorly. As a result, for azines it predicts sizeable charge transfer to solvent with associated red shift for the (n, π^*) absorption in azine–water complexes, followed by a large blue shift associated with the solvation of this complex. The final result is solution solvent shifts which closely parallel the experimental ones, but unfortunately observed spectra for the intermediate azine–water complexes invariably show sizeable blue shifts on cluster formation [54–58]. Hence, the method can reproduce the experimental spectroscopic data to which it was fitted, but this clearly results from a cancellation of large errors associated with each of the individual steps involved.

After studying the azines our next step [17] involved studies of aqueous $Fe^{2+}(H_2O)_6$, and this work is also reviewed in Section 5. This system was chosen as some properties of the liquid structure are known experimentally, as the complex has been investigated thoroughly using accurate intermolecular potential functions, and as its UV absorption spectrum, known for over 60 years, has never been assigned. It involves an interesting metal to solvent charge transfer process which is akin to MLCT except that now the solvent effects are not secondary to the main process but constitute the main process itself, the final chemical product being the evolution of hydrogen gas. While the azine studies looked at MLCT-type processes (i.e. the macroscopic transport of an electron within a molecule) in the limit of weak effects, this study looked at related processes in the limit of extremely strong effects. By establishing that our method works well in these limits, we claim that it should also work reliably for standard MLCT processes (and, of course, for ligand to metal charge transfer and related processes).

Finally, we applied ZHR-SS to quantitatively model MLCT processes in $Ru^{2+}(NH_3)_5$-pyridine, $Ru^{2+}(NH_3)_5$-pyrazine, and $Ru^{2+}(NH_3)_5$-pyrazine-H^+. We conclude that solvent effects change appreciably the nature of MLCT processes in these complexes and dominate the properties observed in electroabsorption experiments. This work is reviewed in Section 6.

2. Basic description of MLCT processes

2.1. Mono-metal complexes

The basic framework in which charge transfer transitions are described is well known [59] and often applied to inorganic MLCT transitions [60]. For simple complexes containing one metal centre this involves considering the interaction of two orbitals, the first being the metal (t_{2g}) atomic orbital of d_π symmetry and the

second the ligand's LUMO molecular orbital. Metal t_{2g} orbitals other than the d_π orbital are weakly interacting [61] and are not normally included in simple models. Initially, the metal d_π and ligand orbitals are separated in energy, with the ligand orbital lying e_0 above the metal orbital. They are then coupled together using an interaction matrix element β. A third parameter r is introduced as the effective distance through which an electron is transferred during the MLCT transition of the uncoupled orbitals, the associated dipole moment change is $\Delta\mu = -er$, where e is the magnitude of the charge on the electron. Naively, as in Eq. (1), one could set r to r_0, the distance between the metal atom and the centre of the ligand; as is shown later, however, this effective distance is modified due to interactions of the MLCT transition with the other ligands on the metal and solvent molecules. Finally, the model MLCT Hamiltonian in the presence of an external field is given by [12,60,62–64]:

$$\boldsymbol{H} = \begin{bmatrix} \mathbf{0} & \beta \\ \beta & e_0 + erF_z \end{bmatrix} \tag{5}$$

where the basis functions depict, in order, the electronic states in which the moving electron is localized on the metal and on the ligand, β is the inter-state electronic coupling, e_0 is the energy difference between the charge-localized states, and F_z is the component of the local applied field in the metal to ligand direction. From this Hamiltonian in the adiabatic approximation [65] the MLCT absorption band properties may be evaluated [12], producing a field-free absorption maximum at

$$h\nu_m = (e_0^2 + 4\beta^2)^{1/2} \tag{6}$$

where h is Planck's constant, transition moment (assuming that two electrons are available for the transition, as appropriate for say a Ru(II) MLCT transition)

$$M = 2^{-1/2} er \left[1 - \left(\frac{e_0}{h\nu_m} \right)^2 \right]^{1/2} \tag{7}$$

and dipole moment change

$$\Delta\mu = -\,\mathrm{sign}(e_0) \times (e^2r^2 - 2M^2)^{1/2} \tag{8}$$

Given experimental M, ν_m, and $\Delta\mu$ it is easy to invert these equations and obtain expressions for the magnitudes of r, e_0, and β:

$$e^2r^2 = (\Delta\mu)^2 + 2M^2 \tag{9}$$

$$e_0^2 = \nu_m^2 \left(1 - \frac{2M^2}{e^2r^2} \right) \tag{10}$$

and

$$\beta^2 = \frac{M^2\nu_m}{2e^2r^2} \tag{11}$$

As stressed and exploited by Cave and Newton [66], Eq. (9) allows an estimate of the effective transfer distance from experimental data, allowing easy correction for

many solvent and correlation effects. The reduction of $\Delta\mu$ below *er* embodied within Eq. (8) arises as a consequence of π back-bonding, the magnitude of which is given by:

$$q_\pi = \frac{4M^2(e^2r^2 - M^2)}{e^3r^4} \tag{12}$$

Within this model, the change in polarizability is predicted to be:

$$\Delta\alpha = -\frac{2M^2}{h\nu_m} \tag{13}$$

i.e. the excited state is predicted to be less polarizable than the ground state. There are, of course, contributions to the polarizability difference that arise from transitions between orbitals not included in this simple model (they are, of course, fully included in ab initio based methods such as ZHR-SS), and these terms always make the excited state more polarizable than the ground state. For small molecules or molecules for which the intervalence transition is very strong and rather low in energy, Eq. (13) is dominant, but this scenario is not common.

Solvent effects on MLCT processes can be separated into those pertaining to ν_m, M, $\Delta\mu$, $\Delta\alpha$, etc. and these can be interpreted in terms of solvent modulation of the chemical parameters e_0, β, and r. The problem is a complex one, however, as the solvent shift $\Delta\nu$ arises to a large part from the differential solvation of the initial and final state dipoles, i.e. is a function of $\Delta\mu$, etc.

2.2. Bis-metal complexes

Inorganic complexes containing two metal centres such as the Creutz–Taube ion have received much attention as they allow for the possibility of intervalence transitions in which an electron is transferred from one metal atom through bridging ligands to the other metal atom; the key issue concerns whether the electronic states of the complex are localized on one of the metal atoms or delocalized over both [65]. In symmetric systems such as $Ru(II)(NH_3)_5$-pyrazine-$Ru(II)(NH_3)_5$, the same issues apply to MLCT transitions: metal to pyrazine MLCT transitions arise from both metal centres, and the excited state could be described alternatively as having either a delocalized Ru(II1/2)–pyrazine$^-$–Ru(II1/2) state or a localized Ru(II)–pyrazine$^-$–Ru(III) state. These possibilities are most easily distinguished by the change in dipole moment $\Delta\mu$ produced on excitation, a localized transition producing a large change while a delocalized transition produces no change at all.

Solvent shifts $\Delta\nu$ are sensitive to $\Delta\mu$ and, for a long time [67], the observed absence of solvent effects has been taken as a strong indication of state delocalization. Direct experimental evidence supporting this link has come from the electroabsorption studies of Oh et al. [11], etc. which directly measure $\Delta\mu$ and $\Delta\nu$ simultaneously. Interpretation of electroabsorption spectra for complexes of this type is quite simple in the limits of either very weak interaction (localization) or very strong interaction (delocalization): in these limits it produces strong 'second

derivative' signals, attributed to $\Delta\mu$, and weak 'first derivative' signals, attributed to $\Delta\alpha$, respectively. For intermediate cases, the net MLCT transition moment is strongly dependent on the antisymmetric metal–ligand stretch coordinate, an effect originating from vibronic coupling acting between the two individual MLCT absorptions. The applied electric field F used in the experiments modulates this vibronic coupling so that the absorption bandshape becomes field dependent, contravening the standard assumption, Eq. (2), used in analysing experimental data. As an example of this effect, a simulated spectrum for the MLCT transition of $Ru(II)(NH_3)_5$-pyrazine is shown in Fig. 1, mapped into that for $Ru(II)(NH_3)_5$–pyrazine–$Ru(II)(NH_3)_5$ using a variety of possible couplings J between the two individual MLCT bands [31]; this is a vibronic coupling calculation, the theory of which, in relation to MLCT spectra, has recently been reviewed [65]. The simulated absorption spectrum narrows as the coupling increases, with a strong, electronically allowed band moving to low frequency while a weak, electronically forbidden band develops and moves to high frequency as $|J|$ increases. Correspondingly, the simulated electroabsorption response changes from a strong classic Liptay 'second derivative' signal at $J = 0$ through a region not describable in a theory embodying Eq. (2) to a weak classic Liptay 'first derivative' signal at $J = 10000\ cm^{-1}$.

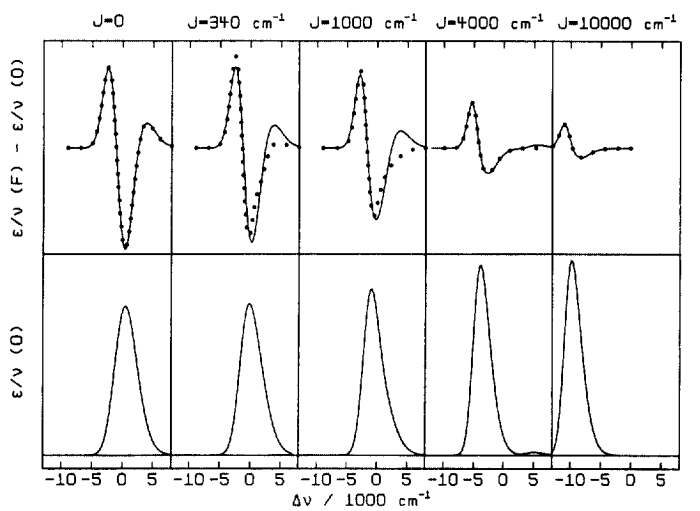

Fig. 1. The lower panels show simulated MLCT absorption bandshapes for $Ru^{2+}(NH_3)_5$–pyrazine–$Ru^{2+}(NH_3)_5$ obtained by vibronically coupling [65] localized $Ru^{2+}(NH_3)_5$-pyrazine MLCT bands at various coupling strengths J, $\Delta\nu$ representing the change in frequency between the monomer and dimer bands. The upper panels show the corresponding calculated changes to the absorption spectra as a function of an applied electric field of magnitude F (solid line), and the best possible fit to this change assuming an invariant bandshape via Eq. (2) (dots). Reproduced with permission from Ref. [31].

3. Qualitative description of solvent effects

The models used to describe MLCT spectra in the previous section involved use of one orbital per metal atom and one ligand orbital. In the broadest sense, 'solvent effects' on the MLCT transition then refers to anything not included in this simple description and includes contributions from other orbitals on the metal and ligand, other (e.g. NH_3) ligands attached to the metal, and interactions of the entire inorganic complex with its surroundings. This produces a powerful conceptual tool useful for viewing the global picture of MLCT transitions as modified by their environment in simple analytical terms. Our initial model [12] was quite successful in interpreting the observed values for the effective separation r; it has been refined and applied to a variety of problems [23]. The major terms include the interaction of the permanent dipole and polarizability of other ligands and solvent molecules with $\Delta\mu$, and the polarization of the MLCT through the interaction of the ligand permanent moments with $\Delta\alpha$. Unfortunately, this approach cannot produce quantitatively accurate results as the interactions between the metal and its ligands are too large to be approximated in this crude, non-self-consistent fashion. In quantitative studies, ZHR-SS thus treats the metal and all its ligands as the chromophore, determining its properties using molecular orbital calculations. The surrounding water molecules thus constitute the solvent, their interactions with the chromophore being treated perturbatively.

Because of hydrogen bonding and other specific interactions, in quantitative calculations the solvation of the complex must itself be treated in a molecular fashion. A qualitative analytical theory for $\Delta\nu$ can be derived for the case in which the solvent is treated as a dielectric continuum with dielectric constant ε and refractive index n in which a non-ionic chromophore resides inside a spherical cavity of radius a. Methods of this type were developed by McRae and others [1–3,5] and described in the most general form by Liptay [6], with the most relevant features extracted by Rettig [7]. The most important contributions to the solvent shift are:

$$\Delta\nu = -\frac{2\varepsilon-2}{2\varepsilon+1}\frac{1}{a^3}\boldsymbol{\mu}\cdot\Delta\boldsymbol{\mu} - \frac{n^2-1}{2n^2+1}\frac{1}{a^3}|\Delta\boldsymbol{\mu}|^2 \tag{14}$$

The first term is usually the largest in magnitude as $|\mu|$ (the initial state dipole moment) is typically much greater than $|\Delta\mu|$ and arises due to the equilibrium polarization induced in the solvent by the solute. The second term arises from the electronic polarization of the solvent adjusting synchronously with the electronic redistribution which occurs in the chromophore. Earlier expressions differ from Eq. (14) in that they introduce crude approximations for the chromophore's polarizability, but general expressions containing $\Delta\alpha$ are available [6,7]. For ionic chromophores, the general picture remains but additional terms must be considered which describe the polarization of the solvent by the ion. The ground state dipole moment μ becomes origin dependent, however, and one must proceed cautiously.

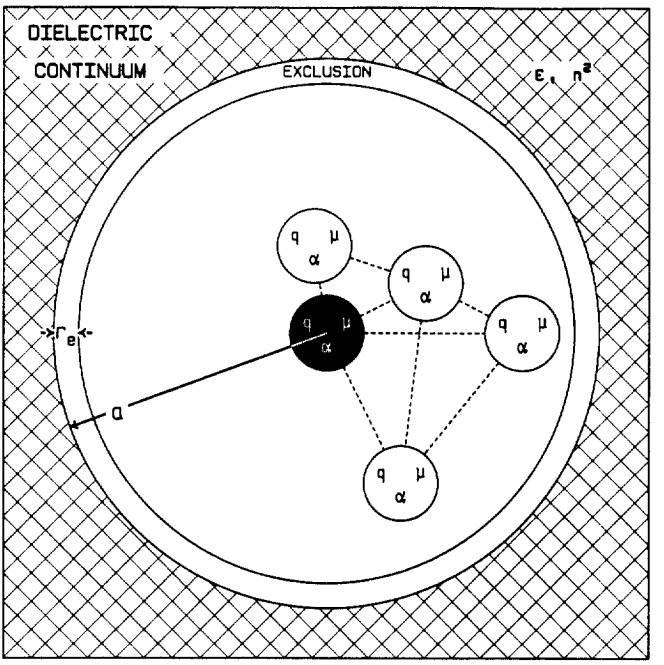

Fig. 2. Key physical features of the calculation of Δv (etc.) averaged over equilibrated liquid configurations including: (1) the chromophore (in black) is represented by a set of electronic state dependent charges q, permanent and induced point dipoles μ, and polarizability centres α; (2) some (typically 100–200) individually represented solvent molecules (in white), similarly described but the permanent moments and charges are electronic state independent with only the induced moments able to respond to changes in the chromophore's electronic state; (3) a small exclusion zone of width r_e; and (4) an outer dielectric continuum of radius a, dielectric constant ε, and refractive index n. The dashed lines indicate some of the specific intermolecular electrostatic interactions.

4. The ZHR-SS computational model for solvent effects on MLCT spectra

To generate a reliable, quantitative scheme for estimating MLCT solvent effects, we consider the metal and all of its ligands as forming the chromophore and treat this in the gas phase using the highest possible level of ab initio calculation. It is then surrounded by a large number (say 100–200) of explicitly represented solvent molecules, and this is then surrounded by a small exclusion zone [68] of radius r_e and then by a dielectric continuum. This is illustrated in Fig. 2. For ruthenium ammine complexes there is no ambiguity as to, in aqueous solution, what molecules are 'ligands' and what molecules are 'solvent'; for other problems such as the solvation of Fe(II) in water [17], however, the inner six water molecules are taken to form part of an $Fe^{2+}(H_2O)_6$ while the solvent water molecules are taken to include only waters beyond this ligand shell.

In principle, the inner layer of explicitly represented solvent molecules is presumed to account for all of the specific interactions between the solvent and solute,

while the dielectric continuum is presumed to account for possible long-range charge–dipole interactions. Such a separation is intuitively necessary as for ionic solutes the long-range interactions are of much greater length scale than will, for a long time, be possible to include in computer simulations. The dielectric cavity is taken to be spherical in shape with radius a, but this assumption does not lead to the introduction of arbitrary parameters as ZHR-SS selects a sufficiently large that the solvent shift is converged. Results obtained for aqueous solvent shifts of (n, π^*) transitions in pyrimidine [16] and MLCT transitions in $Fe^{2+}(H_2O)_6$ [17] and $Ru^{2+}(NH_3)_5$–pyridine [18] shown in Fig. 3 clearly indicate this.

In practice, we have found [16–18] that effects caused by the specific ordering of solvent molecules in the second and third solvent shells away from the chromophore can be quite large. As a consequence, at radii a sufficiently large to include these specific solvation effects, all contributions from the long-range dielectric become insignificant. Hence, in hindsight, inclusion of the long-range contribution often appears to be unnecessary.

The mathematics necessary to describe the dielectric continuum are described in detail elsewhere [16], but in essence involve the use of Friedman image technology [69] with spherical boundary conditions. The equilibrated chromophore in its initial electronic state polarizes the dielectric continuum via image charges and dipoles embedded within it. Standard analytical limits such as Eq. (14), or close approximations thereto, are retrieved in a variety of limits [16] for both ionic and non-ionic chromophores.

ZHR-SS involves two major stages: the generation of representative structures for the solution, and the evaluation of the solvent effects based on those structures. Any available technique may be used for the first stage, provided that it gives

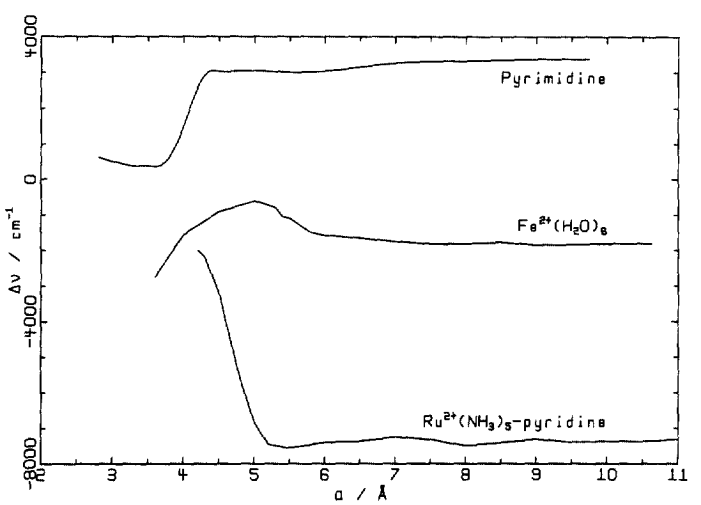

Fig. 3. ZHR-SS calculated solvent shifts $\Delta\nu$ as a function of the dielectric cavity radius a for pyrimidine [16], $Fe^{2+}(H_2O)_6$ [17], and $Ru^{2+}(NH_3)_5$–pyridine [18] in aqueous solution, illustrating the insensitivity of $\Delta\nu$ to the precise number of explicitly included water molecules.

reliable results. We usually perform classical simulations employing effective pair potentials derived [14] using the scheme of Kollman and coworkers [70–73], these being rigid molecule Monte Carlo simulations with the geometry of the complex taken to represent the geometry in solution as accurately as possible. The intermolecular potential functions are generated by combining a standard set of Lennard–Jones potentials with intermolecular electrostatic interactions individually calculated for each isolated chromophore molecule in its initial electronic state (the ground state for an absorption experiment but the excited state for an emission experiment). While potential functions of this type are cumbersome to evaluate compared to canned potential functions, they offer the advantages of greater (and tailorable) accuracy as well as the flexibility to handle excited states. Also, in order to treat the solvent shift reliably, one must first be able to treat the gas-phase spectroscopy reliably, and so the task of determining the chromophore's electronic structure is one which in any case must be completed.

The Lennard–Jones terms used in Kollman's potentials are designed to accompany atomic charges for the solute determined at the ab initio Hartree–Fock self-consistent-field (SCF) level by fitting atomic charges to the molecular electrostatic potential (ESP) outside the molecular van der Waals shell. We have found that this approach gives reasonable results provided that the electronic structure of the solute is described properly at the SCF level. Use of potentials obtained using higher levels of theory, e.g. using multi-configurational SCF (MCSCF), also produces liquid structures that are qualitatively reasonable but overestimate the hydrogen-bond strength and are quantitatively inferior. Clearly, a revised set of Lennard–Jones parameters optimized for use with more accurate solute charge distributions is warranted, but at this stage is unavailable. Indeed, often the SCF electronic structure is qualitatively flawed, making employment of more accurate charge distributions essential [19]. This aspect of our approach constitutes a weakness in that it is not a simple black-box technique in which you dial up the system and obtain the answer. On the other hand, the final solution to any problem will appear well founded as it must simultaneously reproduce a large amount of experimental information ranging from the gas-phase structure of the chromophore to cluster data and the nature of intermolecular interactions to the liquid structure to the effects of solvation. Each of the key steps is essentially individually assessable, with modifications required until they reliably represent their particular feature of the problem.

In the second major stage of ZHR-SS, sampled liquid configurations are processed in order to determine the solvent shift of the absorption band. It is assumed that a significant charge redistribution occurs as a result of the electronic transition, and that the solvent shift arises from the changes in the electrostatic interactions between the solvent and solute (this method is thus clearly inappropriate for the study of $d \rightarrow d$ transitions as these involve essentially no macroscopic charge redistribution [74]). The effects of the solvent on the electronic structure of the solute, and vice versa, are included by treating each molecule as being individually polarizable. This is tantamount to taking the electronic structure of the supramolecular assembly and expressing it self-consistently in terms of a perturbation expan-

sion based on the electronic structures of the individual molecules. The varying properties used to describe the chromophore, the individually represented water molecules, and the dielectric continuum are all depicted in Fig. 2.

The above treatment of polarization is only valid if the perturbation expansion converges quickly. We investigated [20] one complex, $Ru(II)(NH_3)_5$–pyrazine-H^+, in which two molecular orbitals come into resonance; if such a resonance is established by the intermolecular interactions, then a perturbation expansion based on the gas-phase properties would not converge and the electronic structure of the chromophore and solute must then be determined together by ab initio means. For $Ru(II)(NH_3)_5$–pyrazine-H^+, however, the resonance was in fact found to be a gas-phase property and the perturbation expansion remained rapidly convergent.

Charge transfer between the chromophore and solvent molecules is not automatically included, but could be explicitly included in ZHR-SS, if necessary. Test ab initio calculations [16] indicate, however, that solvent effects can be extremely sensitive to small amounts of charge transfer, and that semi-empirical methods such as INDO represent intermolecular charge transfer and hence solvent effects derived from it rather poorly. While solvent-shift calculations using methods such as INDO have been performed [34,35,49], we feel that at present the most reliable method currently available for treating charge transfer effects is to neglect it completely. The results which we have obtained so far (shown later in Table 2) indicate that, while there could possibly be a significant (of order 10%) charge transfer solvent effect on $\Delta\mu$, this contribution is clearly not dominant.

The physical effects on an electronic transition induced by solvation included in ZHR-SS can be summarized: the solvent is initially polarized in equilibrium with the chromophore in its initial electronic state; when the chromophore jumps to its final electronic state, the component of the solvent's polarization attributed to solvent alignment remains fixed and interacts with the chromophore's electronic redistribution, while the component attributed to electronic polarization of the solvent is allowed to re-equilibrate with the chromophore's new electronic structure. Dispersion interactions, believed to contribute on the order of 300 cm^{-1} to most solvent shifts, are not included.

5. Test calculations for ZHR-SS

ZHR-SS is expected to work for any system involving charge transport. Before considering MLCT reactions, we first considered (n, π^*) spectra in azines, in which an electron is taken from a nitrogen lone-pair orbital and placed in the π-LUMO orbital. Compared to MLCT transitions, the electron moves a smaller distance and hence the effects are weaker and harder to model. We also considered a possible metal to solvent cavity transition in aqueous Fe(II) solution, a situation with very strong solvent–solute interactions making it also a more challenging problem.

Table 1
Solvent shifts for azines in aqueous solution

Azine	Method[e]	$\Delta\nu$ (Absorption)		$\Delta\nu$ (Fluorescence)		ΔH	
		Calc.	Obs.	Calc.	Obs.	Calc. ± 2	Obs.[h]
pyridine[a]	SCF	3500	>2500			−13.6	−11.9
pyridazine[b]	CASSCF	4100	3800	800	700	−18.5[f]	−14.9
pyrimidine[c]	SCF	3400	2700	−300	−600	−16.9	−14.3
pyrazine[d]	MRCI	2000	1800	300	700	−16.2[g]	−11.8

$\Delta\nu$ in cm^{-1}, enthalpies of hydration ΔH in kcal mol^{-1}.
[a] Ref. [13]; [b] ref. [21]; [c] refs. [14,16]; [d] ref. [19].
[e] Used to determine the energetic and electrostatic properties of the chromophore in the gas phase.
[f] −16.1 kcal mol^{-1} using SCF-derived potentials.
[g] −13.5 kcal mol^{-1} using SCF-derived potentials.
[h] Ref. [78].

5.1. Azine solutions

These calculations were performed over a number of years and involve the use of different electronic structure methods for determining the gas-phase properties of the chromophores. This variety arose from a combination of factors ranging from technical feasibility limits to the need to get the electronic structure qualitatively correct. Key results for the calculated absorption and fluorescence solvent shifts, $\Delta\nu_A$ and $\Delta\nu_F$, respectively, and for the enthalpy of hydration ΔH are summarized in Table 1. The enthalpies of hydration are systematically too large, especially if post-SCF methods are employed to generate the atomic charges for use in the intermolecular potential functions, and the calculated solvent shifts (using no arbitrarily adjustable parameters) are accurate to ± 700 cm^{-1}. While 700 cm^{-1} is significant for the azines, it is of the order of expected contributions from dispersion effects and is small compared to solvent shifts expected for inorganic MLCT spectra. As detailed individually [15,16,19,21], the calculations do describe a large range of other experimental data adequately, data ranging from solution properties to properties of hydrogen bonded dimeric complexes to high-resolution gas-phase spectroscopic properties of the chromophores. Further, the solvent-shift results are sufficiently accurate to discriminate between various current models for the electronic structures of the azines. For example, the lone pairs in pyrazine have traditionally been described as non-interacting, with (n, π^*) excitation localizing on just one of them (the issue of localized versus delocalized excitations here closely parallels well-known issues in the spectroscopy of inorganic complexes such as the Creutz–Taube ion [65]). This model was based on the interpretation (Eq. (14)) of solvent shift data, and on results of SCF and valence bond electronic structure calculations. An error of interpretation in the original experimental paper [4] (see Ref. [19]) resulted in the observed fluorescence solvent shift being seen to be compatible with a localized description while the observed absorption solvent shift demanded this description. ZHR-SS results [19], on the contrary, show that the

observed absorption shift is compatible with either model while the observed fluorescence shift demands a delocalized model. We showed that only a delocalized model is compatible with the observed gas-phase high-resolution spectra, and that inclusion of dynamic correlation in extensive complete-active-space self-consistent-field (CASSCF) calculations with multi-reference configuration interaction (MRCI) predicts a delocalized structure in the gas phase. Further, we estimated values for the effective coupling J and the reorganization energy and showed that additional solvent contributions to the reorganization energy were not of the correct magnitude to localize the excitation in solution.

5.2. Aqueous Fe(II)

We investigated aqueous Fe(II) [17] as a test system primarily because many computer simulations had already been performed on its structure, these results forming a framework in which we could test ZHR-SS. The accurate simulation of inorganic complexes in water is hampered by various technical problems associated with the presence of ions and the long-range Coulomb forces involved, forces of much longer range than can at present be accommodated in simulations using even the simplest potential functions. We demonstrated that intermolecular potential functions obtained using Kollman's scheme [70–73] treating the ion and its inner coordination shell as a single entity adequately reproduce all experimental and theoretical data available. We also simulated aqueous $Ru^{2+}(NH_3)_6$ [17] and were able to account for all known experimental data for the structure of this solution.

Interestingly, the ultraviolet electronic absorption spectrum of aqueous Fe(II) has never been assigned, despite several decades of intense research [17]. The transition starts at ca. 40000 cm^{-1} and appears to reach a maximum near 50000 cm^{-1} with an extinction coefficient of just 16 l mol^{-1} cm^{-1}, but the remainder of the band (in the vacuum UV) is not yet observed. We considered three of the four suggested mechanisms leading to this absorption, concluding from solvent-shift analysis that it does not arise from iron to ligand–water MLCT. One possibility, however, is that it involves direct transfer of an electron from the metal to a pre-existing cavity located within the solvent. Treating the gas-phase process as the photodetachment of an electron from Fe^{2+}, a process observed at $\nu = 250000$ cm^{-1}, we calculated a solvent shift of -240000 cm^{-1} and an electron confinement kinetic energy of 40000 cm^{-1}, thus predicting a transition energy at 50000 cm^{-1}, as observed. We also estimated the oscillator strength and bandwidth (from the ensemble of water configurations around possible cavities) and found them in agreement with the experimental spectra. While all of the calculations are somewhat crude and, in particular, the intensity may be overestimated so that the observed band intensity could in fact arise from some other source, the location of such a band can be estimated from other means and the calculated solvent shift of -240000 cm^{-1} can be at most in error by ± 10000 cm^{-1}.

6. Results from ZHR-SS for MLCT transitions in Ru complexes

We have studied solvation and solvation effects on MLCT processes in complexes $Ru^{2+}(NH_3)_5$–L with L = pyridine, pyrazine, pyrazine-H^+, and NH_3 using ab initio MCSCF methods to describe the gas-phase electronic structure of the complexes. Key results for the hydrogen bonding, frequency shift $\Delta\nu$, and change in $\Delta\mu$ are shown in Table 2, while hydrogen-bonding radial distribution functions are shown in Fig. 4.

The results for the liquid structure indicate that each ammonia hydrogen is hydrogen-bonded to one water oxygen. Sometimes, one water molecule forms two hydrogen bonds with different ammonia hydrogens so that the total number of water molecules solvating the ammonias is 13 for the hexammine complex and 10–11 for the pentammine complexes. As the radius of this first water coordination shell around the ammonias from the metal is ca. 4 Å (as observed experimentally [18]), and as neat water itself has its second coordination shell at ca. this radius containing 12 water molecules, the density of water molecules near the ion is quite similar to the bulk density. This, plus the similarity of the radial distribution functions in Fig. 4 with those for pure TIP3P water, suggests that the water molecules around the complex do not have enhanced hydrogen bonding or other properties.

Around azine ligands L, no hydrogen bonding is calculated for L = pyridine, one hydrogen bond is calculated to form to the free nitrogen for L = pyrazine, and almost two hydrogen bonds are calculated to form to the acidic hydrogen for L = pyrazine-H^+. This result for L = pyridine is as expected, but those for L = pyrazine differ somewhat from the results of alternate simulations. Using a molecular mechanics potential, Broo [75] found no hydrogen bonding to pyrazine ligand. These simulations considerably overestimate the separation of the water molecules hydrogen-bonded to ammonia (the Ru–O distance is predicted to be ca. 5 Å

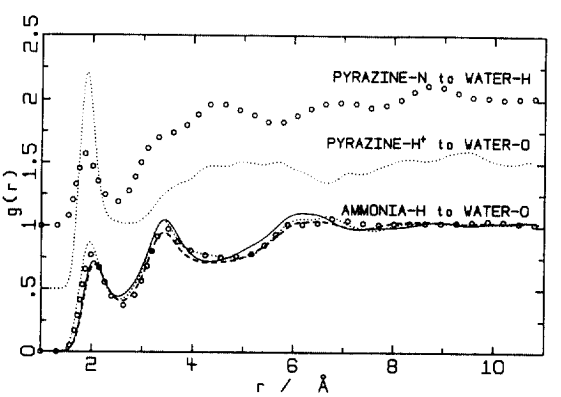

Fig. 4. Intermolecular radial distribution functions $g(r)$ showing hydrogen bonding between the inorganic complexes $Ru^{2+}(NH_3)_5$–L for L = NH_3 (—) [18], pyridine (- - -) [18], pyrazine (◦) [20], and pyrazine-H^+ (···) [20].

Table 2
Solvent effects for complexes $Ru^{2+}(NH_3)_5$-L in aqueous solution

L	Method[d]	ν (Gas)	$\Delta\nu$	ν (Soln.)		$\Delta\mu$ (Gas)	$\Delta\mu$ (Soln.)			# HB per H from NH_3	# HB H_2O to NH_3	# HB to L
				Calc.	Obs.		Calc.	Obs.[c]	Obs.[f]			
NH_3[a]	MCSCF	—	—	—	—	—	—	—	—	1.0	13	—
pyridine[a,c]	MCSCF	38	−8	30	24.5	6[g]	5[g]		3.4	0.9	11	0.0
pyrazine[b]	MCSCF	32.6	−8.3	24.3	21.2	8.8	5.5	4.8 ± 1.3	3.5	0.9	10	1.2
pyrazine-H^+[b]	MCSCF	24.8	−0.5	24.3	18.9	1.0	0.3	<0.3	<1	1.0	10	1.8

$\Delta\nu$ in 1000 cm^{-1}; $\Delta\mu$ in D; # HB are the number of hydrogen bonds per ammonia hydrogen, the total number of water molecules hydrogen-bonded to ammonias, and the number of water molecules hydrogen-bonded to an azine ligand L.

[a] Ref. [18]; [b] ref. [20]; [c] ref. [22].

[d] Used to determine the energetic and electrostatic properties of the chromophore in the gas phase.

[c] Ref. [11] in 50% glycerol–water glass.

[f] Ref. [23] in 50% glycerol–water glass.

[g] Estimated by applying an INDO/S derived geometry relaxation correction to MCSCF results obtained at the calculated gas-phase geometry.

instead of the observed value of ca. 4 Å), and analogous potentials for pyrazine in water also predict no hydrogen bonding, contrary to experiment. It seems that simple molecular-mechanics-type potential functions are not sufficiently flexible to describe correctly the hydrogen-bonding interactions in these systems. Also, X–α density functional calculations by Zhang and Ondrechen [76] predict little charge build-up on the free nitrogen, and simulations using their calculated electronic structure for the complex would very likely also predict no hydrogen bonding. Their results seem inconsistent with the observed increase in basicity of the complex with respect to free pyrazine [18], and again we see that we must have an accurate description of the electronic structure of the solute before we can consider questions concerning solvation.

For L = pyrazine-H^+, one weak and one strong hydrogen bond are predicted to form to the acidic hydrogen atom. No information is available to ascertain the accuracy of this prediction. Naively, one normally expects only one hydrogen bond per hydrogen atom, but this result may be plausible as this hydrogen does bear a substantial charge which could induce multiple solvation.

Note that calculated radial distribution functions and the like are quite sensitive to the boundary conditions used in the simulation [17,18] and care must be taken to obtain sensible results. The structural property which we have found to be the most sensitive is the angular distribution functions for the water molecule hydrogen-bonded to a pyrazine ligand [18]. Presumably, this sensitivity arises because the water molecule in question is quite distant from the Ru atom on which the ionic charge notionally resides: it is the presence of this charge which induces significant boundary effects. This water molecule strongly interacts with the ligand and hence is in a position to influence calculated MLCT properties. We found, however, that calculated variations in its angular distribution did not significantly affect the calculations. All other key hydrogen-bond angular distribution functions were found to be insensitive to boundary effects [17].

For MLCT transitions no gas-phase spectra are available and hence only the final solvent-corrected values may be compared directly with experiment. Accurate calculation of the gas-phase values is itself not a simple task, with methods such as SCF followed by single and double configuration interaction (SDCI) predicting transition energies in error by ca. 50000 cm^{-1} [17]. MCSCF calculation provides the simplest ab initio computational scheme which provides a qualitatively correct description of electronic structures of ground and excited MLCT states, and it is difficult at this stage to estimate absolute reliabilities for computed quantities. The final calculated solution transition frequencies shown in Table 2 are within 6000 cm^{-1} of the observed values, and of the total ca. -8000 cm^{-1} is attributed to solvent shift for L = pyrazine and pyridine and almost none for L = pyrazine-H^+. The result for pyrazine-H^+ is consistent with the observed lack of solvent effect on the transition energy and arises from a resonance between the metal d_π orbital and the ligand's LUMO orbital [77]. Certainly, an error of 5000 cm^{-1} in the ab initio calculation of the gas-phase transition energy is quite plausible and so it is difficult to draw conclusions as to the accuracy of the calculated ca. 8000 cm^{-1} solvent shifts; but based on the results for our test calculations described in Section 5 an error of more than 25% (2000 cm^{-1}) would seem improbable.

The final calculated solution dipole moment changes $\Delta\mu$ shown in Table 2 for L = pyrazine and pyridine are within 2D of the observed values and depict an effective electron-transfer distance r of only one third of the separation r_0 between the metal and ligand centre. This error is ca. 10% of the naive value assuming $r = r_0$ and appears reasonable given the nature of the calculations involved. Also, there exist difficulties in the interpretation of the experimental results due to the need to estimate local-field correction factors. Boxer's results [11] include conservative error bars while Shin et al. [23] have employed some simplistic assumptions in an attempt to reduce this uncertainty. It is certainly possible that the differences between the computed and observed values of $\Delta\mu$ arise from uncertainties in the experimental rather than the computed quantities.

We have shown [17,18,22] that INDO/S provides results of comparable accuracy with the ab initio MCSCF results for the gas-phase transition properties and may be effectively used in this capacity. A modification of the standard INDO/S procedure is necessary, however [18,22], in that the effects of the electronic redistribution associated with MLCT cannot be treated correctly using an empirical parameterization but must be treated explicitly using MCSCF-MRCI techniques, as for ab initio calculations. Alternatively, we have found INDO/S ground state electronic wavefunctions to be not sufficiently accurate for the reliable generation of solvent structures [13–22].

7. Conclusions

The ZHR-SS method has provided considerable insight into solvent effects on MLCT and other electronic transitions involving some degree of electron transfer. Its strength lies in its division of a very complicated problem into small units, each of which can be approached individually at the highest feasible level, and the use of reliable perturbation theory based methods to describe the somewhat weak inter-unit couplings. Thus, we can employ state of the art ab initio methods to accurately describe the ground and excited states of the chromophore in the gas phase, use large simulations with expensive boundary conditions such as Ewald summation to correctly describe the structure of the solvent around the chromophore, and perturbatively evaluate the solvent–solute interaction to determine the solvent effects. Alternate methods which attempt to do all steps at the same time must by necessity introduce severe approximations to the electronic structure of the chromophore and to the liquid structure, and these losses far outweigh the advantages gained by treating the weak solvent–solute interaction non-perturbatively.

Considerable room for improvements to ZHR-SS remain, particularly associated with the desirability of using a consistent high-level ab initio method for determining the electronic structure of the chromophores and linking them into intermolecular potential functions. One aspect of this which has not consistently been properly treated is that the solvent modifies the equilibrium geometry of the solute, and that the electronic structure of the solute needs to be evaluated in the gas phase at the geometry appropriate to the condensed phase. This effect is particularly important

for inorganic complexes for which the relatively weakly held ligands are easily distorted by the solvent. A way to include this is to simply use experimental condensed-phase geometries, but this may not always be possible. An improved version of ZHR-SS could account for this by performing a self-consistent reaction-field calculation for the chromophore not in the gas phase but in some averaged condensed phase. Methods of this type have been shown successful in generating intermolecular potential functions [41], and provide for a more general approach in which solvent shifts calculated assuming no specific solvent interactions could be systematically improved.

Calculated solvent shifts $\Delta\nu$ for MLCT bands for which the ligand is small (e.g. pyrazine) are of the order of $-8000\ cm^{-1}$, but these would grow in magnitude as the charge separation increased. While the shift is significant, there appears to be no qualitative change in the nature of the process due to solvation, with no change even seen for the $Ru^{2+}(NH_3)_5$–pyrazine-H^+ complex, a complex which, in principle, could display solvent-tuned resonance effects.

Nevertheless, electroabsorption experiments [11,23] which depict the MLCT transition in $Ru^{2+}(NH_3)_5$–pyridine and $Ru^{2+}(NH_3)_5$–pyrazine as moving only one quarter of an electron from the metal to the ligand have brought into question our physical insight into just what is involved in MLCT excitations. Our ZHR-SS results have shown that the reduction in the effective number of electrons making the transition is consistent with the view that MLCT involves a one-electron process, and that the cloaking of the number of electrons involved arises as the remainder of the system (ligands, other metal orbitals, solvent molecules) combine to minimize the effects of the electronic transition. The numerical results obtained from the simulations vindicate earlier simple analytical models used to describe this effect [12,23].

Acknowledgements

Assistance from the Australian Research Council is gratefully acknowledged.

References

[1] L. Onsager, J. Am. Chem. Soc. 58 (1936) 1486.
[2] N.S. Bayliss, J. Chem. Phys. 18 (1950) 292.
[3] E.G. McRae, J. Phys. Chem. 61 (1957) 562.
[4] H. Baba, L. Goodman, P.C. Valenti, J. Am. Chem. Soc. 88 (1966) 5411.
[5] V.G. Levich, in: H. Eyring (Ed.), Physical Chemistry an Advanced Treatise IX, Academic Press, New York, 1970, p. 985.
[6] W. Liptay, Z. Naturforsch. 20a (1965) 272.
[7] W. Rettig, J. Mol. Struct. 84 (1982) 303.
[8] M. Kasha, Disc. Faraday Soc. 9 (1950) 14.
[9] K.K. Innes, J.P. Byrne, I.G. Ross, J. Mol. Spectrosc. 22 (1967) 125.
[10] S.G. Boxer, R.A. Goldstein, D.J. Lockhart, T.R. Middendorf, L. Takiff, J. Phys. Chem. 93 (1989) 8280.

[11] D.H. Oh, M. Sano, S.G. Boxer, J. Am. Chem. Soc. 113 (1991) 6880.
[12] J.R. Reimers, N.S. Hush, J. Phys. Chem. 95 (1991) 9773.
[13] J. Zeng, J.S. Craw, N.S. Hush, J.R. Reimers, Chem. Phys. Lett. 206 (1993) 323.
[14] J. Zeng, J.S. Craw, N.S. Hush, J.R. Reimers, J. Chem. Phys. 99 (1993) 1482.
[15] J. Zeng, N.S. Hush, J.R. Reimers, J. Chem. Phys. 99 (1993) 1495.
[16] J. Zeng, N.S. Hush, J.R. Reimers, J. Chem. Phys. 99 (1993) 1508.
[17] J. Zeng, J.S. Craw, N.S. Hush, J.R. Reimers, J. Phys. Chem. 98 (1994) 11075.
[18] J. Zeng, N.S. Hush, J.R. Reimers, J. Phys. Chem. 99 (1995) 10459.
[19] J. Zeng, C. Woywod, N.S. Hush, J.R. Reimers, J. Am. Chem. Soc. 117 (1995) 8618.
[20] J. Zeng, N.S. Hush, J.R. Reimers, J. Am. Chem. Soc. 118 (1996) 2059.
[21] J. Zeng, N.S. Hush, J.R. Reimers, J. Phys. Chem. 100 (1996) 9561.
[22] J. Zeng, N.S. Hush, J.R. Reimers, J. Phys. Chem. 100 (1996) 19292.
[23] Y.K. Shin, B.S. Brunschwig, C. Creutz, N. Sutin, J. Phys. Chem. 100 (1996) 8157.
[24] W. Liptay, in: O. Sinanoglu (Ed.), Modern Quantum Chemistry, vol. III, Academic Press, New York, 1965, p. 45.
[25] W. Liptay, Angew. Chem. Int. Ed. Engl. 8 (1969) 177.
[26] W. Liptay, in: E.C. Lim (Ed.), Excited States, Academic Press, New York, 1974, p. 129.
[27] W. Liptay, Ber. Bunsenges. 80 (1976) 207.
[28] A. Chattopadhyay, S.G. Boxer, J. Am. Chem. Soc. 117 (1995) 1449.
[29] N.S. Hush, J.R. Reimers, J. Phys. Chem. 99 (1995) 15798.
[30] J.R. Reimers, J. Zeng, N.S. Hush, J. Phys. Chem. 100 (1996) 1498.
[31] J.R. Reimers, N.S. Hush, in: K. Prassides (Ed.), Mixed Valence Systems: Applications in Chemistry, Physics, and Biology, Kluwer Academic, Dordrecht, 1991, p. 29.
[32] G.B. Bacskay, J.R. Reimers, in: P. von R. Schleyer (Ed.), Encyclopaedia of Computational Chemistry, Wiley, London, 1998, in press.
[33] F.O. Raineri, H. Resat, B.-C. Perng, F. Hirata, H.L. Friedman, J. Chem. Phys. 100 (1994) 1477.
[34] M.M. Karelson, M.C. Zerner, J. Am. Chem. Soc. 112 (1990) 9405.
[35] M.M. Karelson, M.C. Zerner, J. Phys. Chem. 96 (1992) 6949.
[36] H. Ågren, K.V. Mikkelsen, J. Mol. Struct. 234 (1991) 425.
[37] A. Klamt, G. Schüürmann, J. Chem. Soc. Perkin Trans. 2 (1993) 799.
[38] V. Dillet, D. Rinaldi, J.-L. Rivail, J. Phys. Chem. 98 (1994) 5034.
[39] C.J. Cramer, D.G. Truhlar, in: P. Politzer, J.S. Murray (Eds.), Quantitative Treatment of Solute/Solvent Interactions, Elsevier, New York, 1994, p. 9.
[40] J. Tomasi, M. Persico, Chem. Rev. 94 (1994) 2027.
[41] F. Floris, M. Persico, A. Tani, J. Tomasi, Chem. Phys. Lett. 199 (1992) 518.
[42] A. Broo, S. Larsson, Chem. Phys. 161 (1992) 363.
[43] M.F. Herman, B.J. Berne, J. Chem. Phys. 78 (1983) 4103.
[44] J.R. Reimers, K.R. Wilson, E.J. Heller, J. Chem. Phys. 79 (1983) 4749.
[45] P. Ilich, C. Haydock, F.G. Prendergast, Chem. Phys. Lett. 158 (1989) 129.
[46] R.M. Levy, J.D. Westbrook, D.B. Kitchen, K. Krogh-Jespersen, J. Phys. Chem. 95 (1991) 6756.
[47] J. Aqvist, A. Warshel, Chem. Rev. 93 (1993) 2523.
[48] P.L. Muiño, P.R. Callis, J. Chem. Phys. 100 (1994) 4093.
[49] K.K. Stavrev, M.C. Zerner, T.J. Meyer, J. Am. Chem. Soc. 117 (1995) 8684.
[50] W. Thiel, Adv. Chem. Phys. XCIII (1996) 703.
[51] M. Tuckerman, K. Laasonen, M. Sprik, M. Parrinello, J. Chem. Phys. 103 (1995) 150.
[52] V. Luzhkov, A. Warshel, J. Am. Chem. Soc. 113 (1991) 4491.
[53] S.E. DeBolt, P.A. Kollman, J. Am. Chem. Soc. 112 (1990) 7515.
[54] C. Marzzacco, J. Am. Chem. Soc. 95 (1973) 1774.
[55] R. Rossetti, L.E. Brus, J. Chem. Phys. 70 (1979) 4730.
[56] M.M. Carrabba, J.E. Kenny, W.R. Moomaw, J. Cordes, M. Denton, J. Phys. Chem. 89 (1985) 674.
[57] J. Wanna, J.A. Menapace, E.R. Bernstein, J. Chem. Phys. 85 (1986) 1795.
[58] C.A. Haynam, C. Morter, L. Young, D.H. Levy, J. Phys. Chem. 91 (1987) 2526.
[59] N.S. Hush, Prog. Inorg. Chem. 8 (1967) 391.
[60] A.M. Zwickel, C. Creutz, Inorg. Chem. 10 (1971) 2395.

[61] J.R. Reimers, N.S. Hush, Inorg. Chem. 29 (1990) 3686.
[62] N.S. Hush, M.L. Williams, Chem. Phys. Lett. 5 (1970) 507.
[63] N.S. Hush, M.L. Williams, Chem. Phys. Lett. 6 (1970) 163.
[64] N.S. Hush, M.L. Williams, Theor. Chim. Acta 25 (1972) 346.
[65] J.R. Reimers, N.S. Hush, Chem. Phys. 208 (1996) 177.
[66] R.J. Cave, M.D. Newton, Chem. Phys. Lett. 249 (1996) 15.
[67] N.S. Hush, NATO Adv. Study Inst. Ser. C 58 (1980) 151.
[68] J.A.C. Rullmann, P.Th. van Duijnen, Mol. Phys. 63 (1998) 451.
[69] H.L. Friedman, Mol. Phys. 29 (1975) 1533.
[70] U.C. Singh, F.K. Brown, P.A. Bash, P.A. Kollman, J. Am. Chem. Soc. 109 (1987) 1607.
[71] P. Cieplak, P.A. Kollman, J. Am. Chem. Soc. 110 (1988) 3734.
[72] S.J. Weiner, P.A. Kollman, D.A. Case, U.C. Singh, C. Ghio, G. Alagona, S. Profeta Jr., P. Weiner, J. Am. Chem. Soc. 106 (1984) 765.
[73] S.J. Weiner, P.A. Kollman, D.T. Nguyen, D.A. Case, J. Comput. Chem. 7 (1986) 230.
[74] P. Comba, T. Hambley, Molecular Modelling of Inorganic Systems, VCH, Weinheim, 1995.
[75] A. Broo, Chem. Phys. 174 (1993) 127.
[76] L.-T. Zhang, M.J. Ondrechen, Inorg. Chim. Acta 226 (1994) 43.
[77] R.H. Magnuson, H. Taube, J. Am. Chem. Soc. 97 (1975) 5129.
[78] N.N. Spencer, E.S. Holmboe, M.R. Kirshenbaum, S.W. Barton, K.A. Smith, W.S. Wolbach, J.F. Powell, C. Chorazy, Can. J. Chem. 60 (1982) 1184.